Properties of jet engine combustion particles during the PartEmis experiment: Microphysics and Chemistry

A. Petzold,[1] C. Stein,[1] S. Nyeki,[2] M. Gysel,[2] E. Weingartner,[2] U. Baltensperger,[2]
H. Giebl,[3] R. Hitzenberger,[3] A. Döpelheuer,[4] S. Vrchoticky,[5] H. Puxbaum,[5] M. Johnson,[6]
C. D. Hurley,[7] R. Marsh,[7] and C. W. Wilson[7]

[1] The particles emitted from an aircraft engine combustor were investigated in the European project PartEmis. Measured aerosol properties were mass and number concentration, size distribution, mixing state, thermal stability of internally mixed particles, hygroscopicity, and cloud condensation nuclei (CCN) activation potential. The combustor operation conditions corresponded to modern and older engine gas path temperatures at cruise altitude, with fuel sulphur contents (FSC) of 50, 410, and 1270 $\mu g\ g^{-1}$. Operation conditions and FSC showed only a weak influence on the microphysical aerosol properties, except for hygroscopic and CCN properties. Particles of size D ≥ 30 nm were almost entirely internally mixed. Particles of sizes D < 20 nm showed a considerable volume fraction of compounds that volatilise at 390 K (10–15%) and 573 K (4–10%), while respective fractions decreased to <5% for particles of size D ≥ 50 nm. *INDEX TERMS:* 0305 Atmospheric Composition and Structure: Aerosols and particles (0345, 4801); 0320 Atmospheric Composition and Structure: Cloud physics and chemistry; 0322 Atmospheric Composition and Structure: Constituent sources and sinks; 0365 Atmospheric Composition and Structure: Troposphere—composition and chemistry. **Citation:** Petzold, A., et al., Properties of jet engine combustion particles during the PartEmis experiment: Microphysics and Chemistry, *Geophys. Res. Lett.*, *30*(13), 1719, doi:10.1029/2003GL017283, 2003.

1. Introduction

[2] The role of aviation-related particle emissions in the upper troposphere and lowermost stratosphere is a matter of concern, particularly with respect to a possible effect on the life cycle of cirrus clouds [*Boucher*, 1999]. Despite recent considerable progress in the characterisation of the aerosol particles emitted from jet engines [e.g., *Anderson et al.*, 1998; *Brock et al.*, 2000; *Hagen et al.*, 2001; *Petzold and Schröder*, 1998; *Petzold et al.*, 1999; *Schumann et al.*, 2002] a full picture of their chemical and microphysical properties is still missing.

[3] The overall goal of the European project PartEmis (Measurement and prediction of emissions of aerosols and gaseous precursors from gas turbine engines) was the investigation of the influence of combustor operation conditions and FSC on the microphysical and chemical properties of emitted particles. For these purposes, a combustor which met the ICAO (International Civil Aviation Organisation) engine emissions smoke standard was operated on a test rig at the QinetiQ test site at Pyestock, UK. An extensive set of aerosol measurement methods was employed to achieve as close as possible a consistent and complete data set on the emitted combustion aerosol. An overview of the PartEmis project is given by Wilson et al. (Measurement and Prediction of Emissions of Aerosols and Gaseous Precursors from Gas Turbine Engines (PartEmis): An Experimental Overview, submitted to *Aerospace Sci. Technol.*, 2003).

2. Experimental Approach and Instrumentation

[4] During the experiment, the combustor of the QinetiQ TRACE engine was operated at two different conditions, which were chosen to give the correct modern and older engine gas path temperatures at a cruise altitude of 35,000 ft. The combustor operation parameters for modern (old) conditions were: inlet temperature T_C = 766 (566) K, inlet pressure p_C = 8.3 (7.14) × 10^5 Pa; air fuel ratio = 50.3 (66). The FSC of the burned fuel covered the range from low sulphur fuel (50 $\mu g\ g^{-1}$) to the contemporary average FSC (410 $\mu g\ g^{-1}$), and to a maximum of about three times this average (1270 $\mu g\ g^{-1}$), but still only one third of the amount permitted by current specifications. Conditions are termed ML, MM, MH (OL, OM, OH) for modern (old) conditions and low, medium, and high FSC.

[5] The exhaust gas was sampled using a movable sampling probe which scanned the combustor exit plane to map the lateral distribution of the emissions. Each sampling probe position was maintained for 10 min. The exhaust gas was cooled to a temperature of 425 K by a water-cooled probe and then diluted by a factor of 65. The sample dilution factor was determined from CO_2 mixing ratios measured in the supplied dilution air, diluted and undiluted sample. Data were calculated as exhaust gas density-weighted average values for the entire set of 11 sample probe positions to obtain representative values for each operation condition and FSC. From these average values the influence of combustor operation conditions and FSC on particle microphysical properties and combustor emission characteristics were investigated.

[6] Sample line calibration experiments showed that about 20% by number of the primary combustion aerosol particles were lost to the sample line walls. Data were not

[1]DLR, Institut für Physik der Atmosphäre, Oberpfaffenhofen, Germany.
[2]Paul Scherrer Institut, Villigen, Switzerland.
[3]University of Vienna, Vienna, Austria.
[4]DLR, Institut für Antriebstechnik, Köln, Germany.
[5]Technical University of Vienna, Vienna, Austria.
[6]Reading University, Reading, UK.
[7]QinetiQ, Farnborough, UK.

Table 1. Emission Indices for Mass of Black Carbon (EI_{BC}), Total Carbon (EI_{TC}), Number (EI_{N10}), and Surface (EI_A) of Combustion Aerosol Particles, Specific Surface Area (A), and Smoke Number (SN); Standard Deviations of the Mean are Added in Brackets

	EI_{BC}, g kg^{-1}	EI_{TC}, g kg^{-1}	EI_{N10} [a], 10^{14} kg^{-1}	EI_A [b], m^2 kg^{-1}	A, m^2 g^{-1}	SN
OL	0.070 (0.008)	0.089 (0.028)	5.7 (0.9)	5.5 (0.9)	79	13.4
OM	0.051 (0.005)	0.090 (0.029)	7.5 (0.6)	5.8 (0.5)	114	9.8
OH	0.081 (0.016)	0.125 (0.040)	15.8 (1.4)	11.6 (1.1)	143	15.1
ML	0.043 (0.005)	0.044 (0.011)	3.7 (0.3)	4.2 (0.4)	98	12.2
MM	0.028 (0.003)	0.069 (0.020)	2.7 (0.3)	2.4 (0.2)	86	7.5
MH	0.054 (0.006)	0.104 (0.034)	7.0 (1.7)	5.6 (1.4)	127	12.6

[a]Refers to particles of size D $\geq$ 10 nm.
[b]Surface area was calculated from measured size distributions.

corrected for sampling line losses because relative changes in the emission properties between different operation conditions and FSC were the major objectives of PartEmis. All data are either reported as concentration values referring to standard conditions (T = 273.14 K, p = 1013.25 hPa) of the undiluted sample gas, or as an emission index in terms of an emitted quantity per kg of consumed fuel.

[7] The standard test rig instrumentation available at the QinetiQ test bed covered gaseous compounds CO, CO_2, total hydrocarbons (HC), NO_x, and smoke. The black carbon (BC) mass concentration in the diluted sample gas was measured by a Particle Soot Absorption Photometer applying the recommended corrections (PSAP; *Bond et al.* [1999]). The specific absorption cross section at $\lambda =$ 0.55 μm, $\sigma_{abs} = 7$ m^2 g^{-1} [*Petzold and Schröder*, 1998] was used for conversion of light absorption to BC mass. Instrument calibration studies during PartEmis confirm this value. The number concentrations were measured in the size intervals D = 4–7 nm, 7–9 nm, 9–21 nm, and 21–250 nm with parallel-operated Condensation Particle Counters which were set to different lower instrument cut-off diameters (Condensation Particle Size Analyser, CPSA, [*Stein et al.*, 2001]). Particles of size D > 9 nm which are detected in CPSA channels 3 and 4, are in the following referred to as N_{10}. Particle size distributions were measured with a commercial Scanning Mobility Particle Sizer (SMPS; TSI Model 3071) and a Volatility-Tandem Differential Mobility Analyser (V-TDMA) in the size range D > 13 nm.

[8] The aerosol mixing state and the thermal stability of the combustion aerosol were determined with thermal denuder methods [*Burtscher et al.*, 2001]. Setting the denuder temperatures to 390 K and 573–625 K, respectively, distinguishes sulphuric-acid like matter (vaporises at 390 K) from matter of higher thermal stability (vaporises between 390 and 573 K), and from refractory BC-like material. The thermal treatment of almost monodisperse particle size fractions which were preselected by a DMA provides information whether the aerosol is internally or externally mixed. The ratio of diameters after and before thermal treatment yields the particle shrinkage factor D^3/D_0^3 which describes the particle volume reduction by the thermal treatment. The hygroscopic particle growth factor under subsaturated conditions was measured with a Hygroscopicity Tandem DMA. The activated cloud condensation nuclei (CCN) were measured at a super-saturation of 0.7%. The chemical composition of the carbonaceous fraction in terms of total carbon (TC) and elemental carbon (EC) of the

exhaust particles was determined using multi-step combustion methods.

3. Results and Discussion

[9] The emitted aerosol was composed of primary carbonaceous particles forming inside the combustor, and of condensation particles nucleating in the cooling exhaust gas from gaseous precursors. The emission properties with respect to the primary aerosol are compiled in Table 1 in terms of BC mass (EI_{BC}), TC mass (EI_{TC}), number (EI_{N10}), and surface area (EI_A) emissions per kg of consumed fuel, and smoke number. The number emission index EI_{N10} refers to particles of sizes D $\geq$ 10 nm. The surface emission index EI_A was calculated from measured size distributions. When operated at old engine conditions, EI_{BC} varies from 0.051 to 0.081 g kg^{-1}. Operated at modern engine conditions, EI_{BC} ranges from 0.028 to 0.054 g kg^{-1} which is a factor of < 2 lower, while the variation in EI_{TC} is less pronounced. Similar relations hold for the other properties. However, the amount of emitted particulate matter is within the range permitted by the ICAO rules in all cases. The specific surface area A per gram of particulate matter is approximately 100 m^2 g^{-1}. PartEmis emission indices for the medium FSC case are shown in Figure 1 together with mass and number emission indices from various in-flight studies. The order of aircraft types on the y-axis corresponds to an increasing engine certification year from bottom to top. The PartEmis emission indices fit well into this picture and represent a range of engines which are currently in use.

[10] Mean particle sizes were determined as count median diameter *CMD* and diameter of average mass *AMD* by Differential Mobility Sizing methods (SMPS), and calculated from simultaneously measured BC mass concentrations c_{BC} and number concentrations N_{10} (D $\geq$ 10 nm). The mean diameter of the emitted combustion particles depends only very weakly on the combustor inlet temperature and on the FSC (see Figure 2). The values of particle diameters deviate from each other depending on the method, but overall trends are similar. Assuming a mass density of 1.0 g cm^{-3} and spherical particle shape, a good agreement between the *AMD*
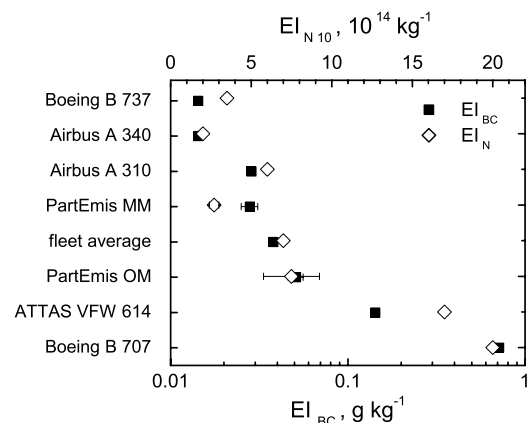
Figure 1. Particle emission characteristics of the PartEmis combustor operated with medium FSC, plotted in the context of emission characteristics measured for aircraft at cruise conditions [*Petzold et al.*, 1999; *Schumann et al.*, 2002].
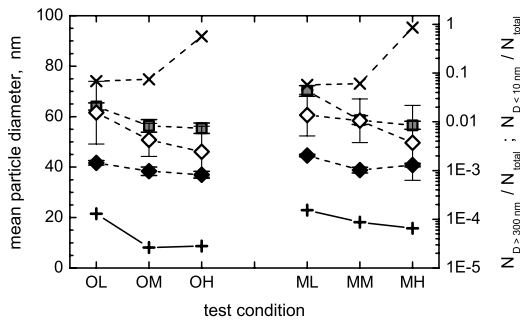
Figure 2. Test-condition averaged diameters of emitted combustion aerosol particles: count median diameter *CMD* measured with a Differential Mobility Analyzer (filled diamonds), diameter of average mass, *AMD*, calculated from measured size distributions (filled squares), and calculated from measured mass and number concentrations (open diamonds), respectively, fraction of particles larger than 300 nm (+) and smaller than 10 nm (×) in diameter.

values calculated from size distributions and calculated from mass and number concentration data is found. Scanning electron microscope pictures confirm the very compact shape of aircraft engine generated sub-100-nm combustion particles [*Döpelheuer amd Wahl*, 2001]. Mean *CMD* values are 37−41 nm for old engine and 39−45 nm for modern engine conditions. The geometric standard deviation of the size distribution is 1.69 (1.66−1.73) in both cases.

[11] As shown in Figure 2 particles smaller than 10 nm contribute less than 10% of the total exhaust aerosol in the low and medium FSC cases. Burning fuel with high FSC, the formation of condensation particles is observed in the size range $D < 10$ nm. In this case, sub-10-nm particles contribute up to 85% by number to the total emitted aerosol. The vast majority of sub-10-nm particles is assumed to form by homogeneous nucleation of condensable gases at the sample dilution point where the hot sample gas is mixed with cold dilution air. A similar process takes place in the cooling plume of an aircraft engine at cruise altitudes [e.g., *Brock et al.*, 2000].

[12] *Hagen et al.* [2001] investigated the particle emissions from an engine with varying combustor inlet temperature T_C at simulated altitude conditions. They also report a gradual increase in particle size with increasing T_C and an increase in particle emissions for an increasing FSC. Observations reported from engine test studies at ground conditions [*Petzold and Schröder*, 1998; *Petzold and Döpelheuer*, 1998] and in-flight [*Schumann et al.*, 2002] support the weak increase in emissions of primary particles with increasing FSC.

[13] The mixing state of particles in selected size bins was analysed in order to investigate how far condensation particles extend into the size range of primary carbonaceous particles. The fraction of refractory particles of the exhaust aerosol is 0.99 ± 0.01 for $D = 30 \pm 2$ nm and 1.00 ± 0.01 for $D = 80 \pm 3$ nm for all test conditions. Neither the combustor operation conditions nor the FSC seem to influence the mixing state of the exhaust aerosol in the size range $D \geq 30$ nm which is entirely internally mixed.

[14] The fraction of refractory particles of the total aerosol is shown in Figure 3 for the size bin $D = 15 \pm 1$ nm as probe position averages for the high FSC cases when strong
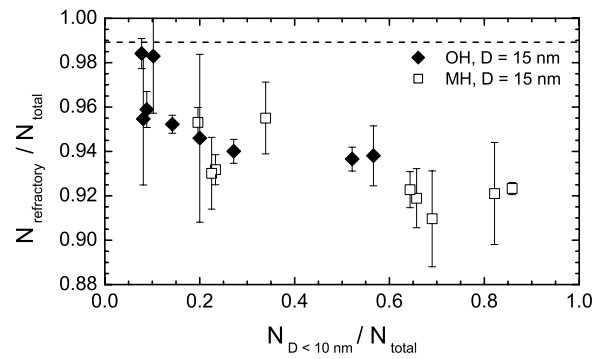

Figure 3. Fraction of refractory particles (T = 625 K) of the total aerosol as a function of the fraction of ultrafine particles of size D < 10 nm of the total aerosol for sizes D = 15 nm (symbols) and D ≥ 30 nm (dashed line).

formation of condensation particles was observed. The variation in condensation particle formation at constant FSC was caused by a variation of the amount of emitted carbonaceous particles at different combustor exit plane sections. The fraction of refractory particles in this size bin is inversely correlated to the fraction of sub-10 nm condensation particles. Hence, a small fraction of condensation particles grows into the size range $D \leq 15$ nm (relative humidity <10%) and generates a very small externally mixed fraction of <5% by number. This fraction of externally mixed condensation particles vanishes in larger size bins because the particle growth is limited to very small particle sizes.

[15] The volume shrinkage factor D^3/D_0^3 of the internally mixed particles decreases with decreasing particle size at each FSC level (see Figure 4). The fraction of thermally less stable particulate matter that volatilises at 390 K increases from 1−2% for low FSC to approx. 5% for high FSC for particles of D > 50 nm. An additional fraction of matter that volatilises at 573 K is not observed for low FSC, but for medium and high FSC another 3−5% by volume are removed at 573 K. Thermally less stable compounds contribute up to max. 15% by volume to particles smaller than 30 nm. At denuder temperatures of 573 K, another 10% by volume of material are removed from sub-30 nm particles.

[16] The hygroscopic growth of particles is measured by the Hygroscopicity Tandem DMA [*Gysel et al.*, 2003] as a
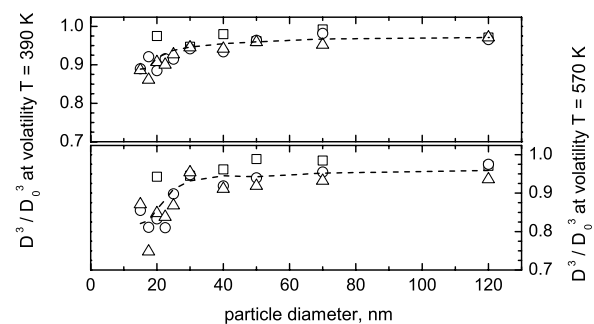
Figure 4. Particle volume shrinkage factors (D^3/D^3_0) for modern engine combustor conditions at denuder temperatures $T = 390$ K and $T = 570$ K for low FSC (squares), medium FSC (circles) and high FSC (triangles); dashed lines represents a 3-point running mean over all FSC at the respective temperatures.

function of particle size. It is found that the hygroscopic growth of particles increases with increasing FSC and decreases with increasing particle size. This behaviour shows similar trends as the thermally less stable fraction of particles.

[17] First chemical analyses of particulate matter using multiple step combustion methods [*Schmid et al.*, 2001] show that the carbonaceous fraction is composed of about 80–90% BC for low FSC and 40–65% for low ad medium FSC. The combustor temperature has no significant effect on the BC fraction of TC. The thermally less stable fraction of particles can very likely be attributed to adsorbed sulphuric acid, since it increases with increasing FSC. However, also partially oxidised hydrocarbon compounds and residuals from unburned fuel may also contribute to this fraction. The fraction of higher thermal stability is primarily composed of organic matter which contributes a substantial part to the carbonaceous material.

[18] The ability of combustion particles to form CCN at a saturation ratio of 1.007 was also investigated [*Hitzenberger et al.*, 2003]. The fraction of activated particles increases from $7-9 \times 10^{-4}$ at low FSC to $1.4-3 \times 10^{-3}$ at medium FSC and $5-8 \times 10^{-3}$ at high FSC. Increasing the FSC by a factor of 25 increases the CCN fraction by a factor of 5 (old conditions) and 12 (modern conditions), respectively. Particles larger than about 300 nm can undergo a Kelvin-type activation at the given conditions. As this size fraction decreases with increasing FSC (see Figure 2), an influence of the particle size on the CCN activation can be excluded. The observed effect can thus be attributed to modifications in the surface properties of the particles by adsorbed sulphuric acid or organic matter.

4.　Summary and Conclusions

[19] The primary aerosol emitted from the combustor has a lognormal size distribution centred at a $CMD = 40 \pm 3$ nm of width $GSD = 1.69 \pm 0.03$. No significant differences in particle size distribution are observed between old and modern engine operation conditions and different FSC levels. When burning high FSC fuel, a strong formation of condensation particles is favoured which grow into a size range $D < 10$ nm. In the absence of condensation particle formation, less than 10% of the particles are smaller than 10 nm, while the fraction of large-sized particles with $D > 300$ nm is of the order of 10^{-4} in all cases.

[20] The presented results indicate, that the emitted aerosol is almost entirely internally mixed in the size range $D > 10$ nm. These results are in contradiction to previous in-flight studies [e.g., *Anderson et al.*, 1998; *Petzold et al.*, 1999] where about 12–16% of particles larger than 10 nm were observed to be thermally unstable. However, since the sample air during the PartEmis measurements was quite dry (RH < 30%), condensation particles cannot grow by water uptake but remain very small in size, which may explain the observed discrepancy.

[21] The results from the analyses of mixing state and composition of the emitted combustion aerosol agree with observations of water uptake properties [*Gysel et al.*, 2003] and CCN activation [*Hitzenberger et al.*, 2003]. Increasing the FSC results in increased hygroscopic growth of particles ≤ 100 nm and in a higher CCN concentration in the exhaust gas (at 0.7% supersaturation).

[22] The PartEmis data base on size distribution, mixing state, thermal stability, hygroscopic growth factors and CCN activation provides relevant information for the investigation of the ability of aviation-related particles to influence cloud formation in the atmosphere, and hence to contribute to a better understanding of climate impact of aviation.

References

Anderson, B. E., et al., Airborne observations of aircraft aerosol emissions, I, Total nonvolatile particle emission indices, *Geophys. Res. Lett.*, *25*, 1689–1692, 1998.

Bond, T. C., T. L. Anderson, and D. Campbell, Calibration and intercomparison of filter-based measurements of visible light absorption by aerosols, *Aerosol Sci. Technol.*, *30*, 582–600, 1999.

Boucher, O., Influence of air traffic on cirrus occurrence, *Nature*, *397*, 30–31, 1999.

Brock, C. A., et al., Ultrafine particle size distributions measured in aircraft exhaust plumes, *J. Geophys. Res.*, *105*, 26,555–26,567, 2000.

Burtscher, H., et al., Separation of volatile and non-volatile aerosol fractions by thermodesorption: Instrumental development and application, *J. Aerosol Sci.*, *32*, 427–442, 2001.

Döpelheuer, A., and C. Wahl, Determination of quantities and properties of aircraft engine generated soot, in, *Aviation, aerosols, contrails and cirrus clouds*, edited by U. Schumann, and G. Amanatidis, Air pollution research report 74, pp 91–94, European Commission, Brussels, 2001.

Gysel, M., S. Nyeki, E. Weingartner, U. Baltensperger, H. Giebl, R. Hitzenberger, A. Petzold, and C. W. Wilson, Properties of jet engine combustion particles during the PartEmis experiment: Hygroscopicity at subsaturated conditions, *Geophys. Res. Lett.*, *30*(11), 1566, doi:10.1029/2003GL016896, 2003.

Hagen, D. E., P. D. Whitefield, J. D. Paladino, and O. Schmid, Comparative study of jet engine combustion emissions and engine operating conditions, in *Aviation, aerosols, contrails and cirrus clouds*, edited by U. Schumann and G. Amanatidis, Air pollution research report 74, pp 106–110, European Commission, Brussels, 2001.

Hitzenberger, R., H. Giebl, A. Petzold, M. Gysel, S. Nyeki, E. Weingartner, U. Baltensperger, and C. W. Wilson, Properties of jet engine combustor particles during the PartEmis experiment. Hygroscopic properties at supersaturated conditions, *Geophys. Res. Lett.*, doi:10.1029/2003GL017294, 2003.

Petzold, A., and A. Döpelheuer, Reexamination of black carbon mass emission indices of a jet engine, *Aerosol Sci. Technol.*, *29*, 355–356, 1998.

Petzold, A., and F. P. Schröder, Jet engine exhaust aerosol characterization, *Aerosol Sci. Technol.*, *28*, 62–76, 1998.

Petzold, A., A. Döpelheuer, C. A. Brock, and F. P. Schröder, In situ observations and model calculations of black carbon emission by aircraft at cruise altitude, *J. Geophys. Res.*, *104*, 22,171–22,181, 1999.

Schmid, H., et al., Results of the "carbon conference" international aerosol carbon round robin test stage I, *Atmos. Environ.*, *35*, 2111–2121, 2001. (the employed method refers to Laboratory 9)

Schumann, U., F. Arnold, R. Busen, J. Curtius, B. Kärcher, A. Kiendler, A. Petzold, H. Schlager, F. Schröder, and K.-H. Wohlfrom, Influence of fuel sulfur on the composition of aircraft exhaust plumes: The experiments SULFUR 1–7, *J. Geophys. Res.*, *107*(D15), 4247, doi:10.1029/2001JD000813, AAC 2-1-AAC 2-27, 2002.

Stein, C., F. Schröder, and A. Petzold, The Condensation Particle Size Analyzer: A new instrument for the measurement of ultrafine aerosol size distributions, *J. Aerosol Sci.*, *32*, S381–S382, 2001.

————————————
A. Petzold and C. Stein, DLR, Institut für Physik der Atmosphäre, Oberpfaffenhofen, Germany. (andreas.petzold@dlr.de)

S. Nyeki, M. Gysel, E. Weingartner, and U. Baltensperger, Paul Scherrer Institut, Villigen, Switzerland.

H. Giebl and R. Hitzenberger, University of Vienna, Vienna, Austria.

A. Döpelheuer, DLR, Institut für Antriebstechnik, Köln, Germany.

S. Vrchoticky and H. Puxbaum, Technical University of Vienna, Vienna, Austria.

M. Johnson, Reading University, Reading, UK.

C. D. Hurley, R. Marsh, and C. W. Wilson, QinetiQ, Farnborough, UK.